ELSEVIER

Edge-unfolding nested polyhedral bands [☆]

Greg Aloupis [a,*,1], Erik D. Demaine [b,2], Stefan Langerman [c,3], Pat Morin [d,1],
Joseph O'Rourke [e,4], Ileana Streinu [e,5], Godfried Toussaint [a,1]

[a] *School of Computer Science, McGill University, Canada*
[b] *MIT Computer Science and Artificial Intelligence Laboratory, USA*
[c] *Département d'Informatique, Université Libre de Bruxelles, Belgium*
[d] *School of Computer Science, Carleton University, Canada*
[e] *Department of Computer Science, Smith College, USA*

Abstract

A *band* is the intersection of the surface of a convex polyhedron with the space between two parallel planes, as long as this space does not contain any vertices of the polyhedron. The intersection of the planes and the polyhedron produces two convex polygons. If one of these polygons contains the other in the projection orthogonal to the parallel planes, then the band is *nested*. We prove that all nested bands can be *unfolded*, by cutting along exactly one edge and folding continuously to place all faces of the band into a plane, without intersection.
© 2007 Elsevier B.V. All rights reserved.

Keywords: Polyhedra; Folding; Slice curves

1. Introduction

It has long been an unsolved problem to determine whether every polyhedron may be cut along edges and unfolded flat to a single, non-overlapping polygon [6,7,9,12]. An interesting special case emerged in the late 1990s:[6] can the
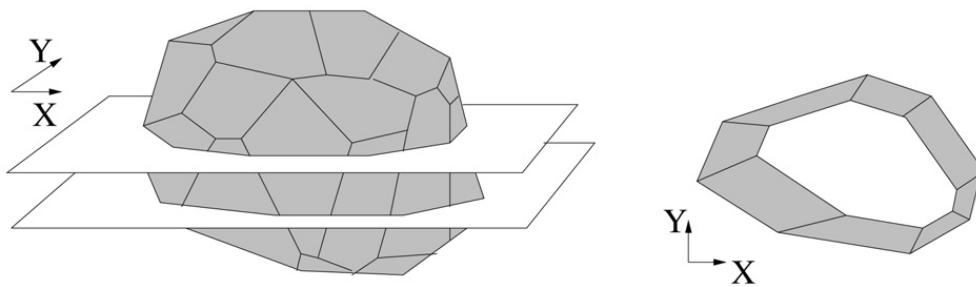
Fig. 1. A polyhedron cut by two parallel planes, and the projection of the resulting band onto the xy plane.
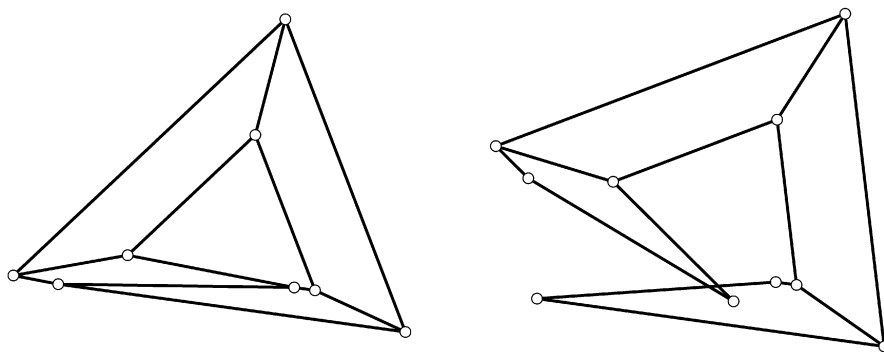

Fig. 2. Projection of a band that self-intersects when cut along the wrong edge and unfolded. Left: original band. Edges at the bottom are nearly collinear. Right: self-intersecting unfolding.

band of surface of a convex polyhedron enclosed between parallel planes, and containing no polyhedron vertices, be unfolded without overlap by cutting an appropriate single edge? A band and its associated polyhedron are illustrated in Fig. 1.

This band forms the side faces of what is known as a *prismatoid* (the convex hull of two parallel convex polygons in $\mathbb{R}^3$) but the band unfolding question ignores the top and bottom faces of the prismatoid. An example was found (by E. Demaine and A. Lubiw) that shows how flattened bands can end up overlapping if a "bad" edge is chosen to cut; see Fig. 2.

Band-like constructs have been studied before. Bhattacharya and Rosenfeld [3] define a polygonal *ribbon* as a finite sequence of polygons, not necessarily coplanar, such that each pair of successive polygons intersects exactly in a common side. Triangular and rectangular ribbons (both open and closed) have also been studied. Arteca and Mezey [2] deal with continuous ribbons. Simple bands can be used as linkages to transfer mechanical motion, as pointed out by Cundy and Rollett [5]. Open and closed rings of rigid panels connected by hinges have also been considered in robotics as another model for robot arms with revolute joints. For example, their singularities are well understood mathematically [4]. As a special case of the more general *panel-and-hinge* structures studied in rigidity theory, they are relevant to protein modeling [13]. In all these instances, almost no attention was paid to questions regarding their non-self-intersecting states or their self-collision-avoiding motions.

There is one unfolding result that is particularly relevant to our problem, which may be interpreted as unfolding infinitely thin bands. This result states that a *slice curve*, the intersection of a plane with a convex polyhedron, develops (unfolds) in the plane without overlap [8,10]. This result holds regardless of where the curve is cut. Thus, both the top and the bottom boundary of any band (and in fact any slice curve between) cannot self-intersect after a band has been flattened. So overlap can only occur from interaction with the cut edge, as in Fig. 2.

Here we will prove that a particular type of band can be unfolded by explicitly identifying an edge to be cut. A band is *nested* if projecting the top boundary A orthogonally onto the plane of the bottom boundary B results in a polygon nested inside B. For example, the band in Fig. 1 is nested. Intuitively, we might expect to obtain a nested band if both parallel planes cut the polyhedron near its "top". We prove that all nested bands can be unfolded. Our proof provides more than non-overlap in the final planar state: it ensures non-intersection throughout a continuous unfolding motion.

2. Bands

We first define bands more formally and analyze their combinatorial and geometric structure, without regard to unfolding.

Let P be the surface of a convex polyhedron with no coplanar faces. Let $z_0, z_1, \ldots, z_m$ denote the sorted z coordinates of the vertices of P. Pick two z coordinates z_A and z_B that fall strictly between two consecutive vertices z_i and z_{i+1}, and suppose that z_A is above z_B: $z_i < z_B < z_A < z_{i+1}$. The *band* determined by P, z_A, and z_B is the intersection of P's surface with the horizontal slab of points whose z coordinates satisfy $z_B \leqslant z \leqslant z_A$.

The band is a polyhedral surface with two components of boundary, called A and B. Specifically, we define A as the *top (polygonal) chain* of the band, i.e., the intersection of P's surface with the plane $z = z_A$, and B is the *bottom chain*, corresponding to the plane $z = z_B$. Both chains A and B are convex polygons in their respective horizontal planes, being slice curves of a convex polyhedral surface P. All vertices of the band are vertices of either A or B.

Every vertex of the band is incident to exactly three edges: two along the chain A or B containing the vertex, and the third connecting to the other chain. This third edge, called a *hinge*, is part of an edge of the original polyhedron P connecting a vertex of P with z coordinate less than z_B to a vertex of P with z coordinate greater than z_A. The hinge from each vertex of the band defines a perfect matching between vertices of the top chain A and vertices of the bottom chain B. This matching is consistent with the cyclic orders of A and B in the sense that, if vertex a_i of A is paired with vertex b_i of B, then the vertex a_{i+1} clockwise around A from a_i is paired with the vertex b_{i+1} clockwise around B from b_i. This correspondence defines a consistent clockwise labeling of the vertices $a_0, a_1, \ldots, a_{n-1}$ of A and the vertices $b_0, b_1, \ldots, b_{n-1}$ of B, unique up to a common cyclic shift.[7]

Each face of the band is a quadrilateral spanned by two adjacent vertices a_i and a_{i+1} on the top chain A and their corresponding vertices b_i and b_{i+1} on the bottom chain B. This facial structure follows from the edge structure of the band. Each face is planar because it corresponds to a portion of a face of the original polyhedron P. Because edges $a_i a_{i+1}$ and $b_i b_{i+1}$ lie in a common plane as well as in parallel horizontal planes, the edges themselves must be parallel. Thus every face of the band is in fact a trapezoid, with parallel top and bottom edges.

3. Nested bands

Next we analyze the geometric structure of nested bands in particular, still without regard to unfolding.

A band is *nested* if the orthogonal projection of A into the xy plane is strictly contained inside the orthogonal projection of B into the xy plane. (Of course, a band is just as nested if instead B's projection is contained inside A's projection, but in that case we just reflect the band through the xy plane.)

Nested bands have a particularly simple structure when projected into the xy plane. As with all bands, each face projects to a trapezoid. The unique property of a nested band is that none of its edges cross in projection. This property follows because the projected edges are a subset of a triangulation of the projections of A and B, which themselves do not intersect by the nested property. (In non-nested bands, edges of A intersect edges of B in projection.) Thus the projected trapezoidal faces of the band form a planar decomposition of the region of the xy plane interior to the projection of B and exterior to the projection of A. When dealing with projections, we will refer to A (B) as the *inner (outer) chain*.

In the xy projection, the *normal cone* of a vertex a_i of A (or more generally any convex polygon) is the closed convex region between the two exterior rays that start at a_i and are perpendicular to the incident edges $a_{i-1} a_i$ and $a_i a_{i+1}$ respectively. See Fig. 3. The two rays forming this cone decompose the local exterior of A around a_i into three regions: left (counterclockwise), inside, and right (clockwise) of the normal cone.

Lemma 1. *In the xy projection of a nested band, not all hinges $a_i b_i$ can be to the right (or all to the left) of the normal cones of their inner endpoint a_i.*

Proof. The following proof refers exclusively to the xy projection. Suppose by symmetry that all hinges are clockwise (right), or on the right border, of their respective normal cones on the inner chain A. For each i, define T_i to be the

---

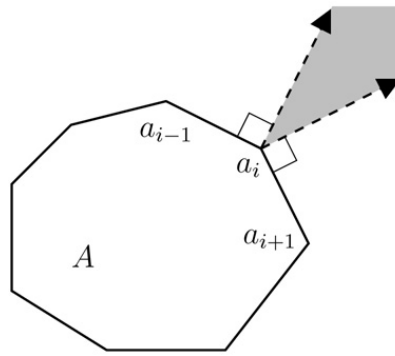[7] Throughout this paper, indices are taken modulo n.
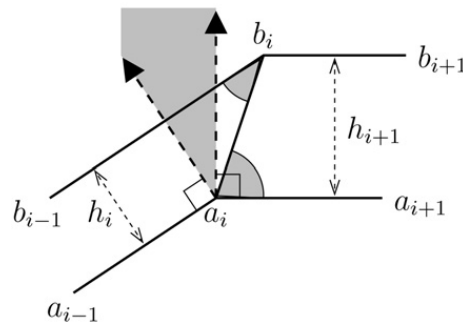
Fig. 3. The normal cone of a vertex a_i.

Fig. 4. If the hinge $a_i b_i$ is right of the normal cone at a_i, then the top shaded angle is less than the bottom shaded angle, so $h_i < h_{i+1}$.

trapezoid with vertices $a_{i-1}, a_i, b_i, b_{i-1}$, and let h_i denote its height, i.e., the distance between the opposite parallel edges $a_{i-1}a_i$ and $b_{i-1}b_i$. See Fig. 4. Because $a_i b_i$ is right of the perpendicular at a_i to $a_i a_{i+1}$, and because the interior angle at b_i is convex, the convex angle $a_i b_i b_{i-1}$ is less than the convex angle $b_i a_i a_{i+1}$. Thus, the height h_i of T_i is less than the height h_{i+1} of the clockwise next trapezoid T_{i+1}. Applying this argument to every T_i, we obtain a cycle of strict inequalities $h_0 < h_1 < \cdots < h_{n-1} < h_0$, which is a contradiction. $\square$

4. Opening convex chains

Before we study the unfolding of bands, we first study what happens when opening a convex closed chain (polygon) by cutting it at some vertex a_i and increasing all other internal angles.

We introduce some basic notation and terminology for a convex closed chain; refer to Fig. 5(a). Given a clockwise-oriented convex closed chain $A = \langle a_0, a_1, \ldots, a_{n-1} \rangle$ in the plane, the *interior angle* α_j at a vertex a_j, $0 \leqslant j \leqslant n - 1$, is the angle $a_{j-1}a_j a_{j+1}$ located on the right side of the chain. Let $\tau_j = \pi - \alpha_j$ be the *turn angle* at a_j, which is positive (to the right) because of the clockwise orientation of A. Let θ_j be the counterclockwise angle of the vector $a_j - a_{j-1}$ from the positive x axis. If $a_i - a_{i-1}$ is fixed along the positive x axis, then for a chain with all right turns, we have $\theta_i = 0$, $\theta_{i-1} = \tau_{i-1}$, and in general,

$$\theta_{i-k} = \sum_{j=i-k}^{i-1} \tau_j. \tag{1}$$

An *opening* of a convex closed chain A at a_i is a motion $A'(t)$ that cuts the chain at a_i, holds the edge $a_{i-1}a_i$ fixed, and monotonically increases all other interior angles. See Fig. 5(b). More precisely, an opening of A at a_i consists of a non-strictly increasing function $\delta_j : [0, 1] \to [0, \tau_j]$, with $\delta_j(0) = 0$, for each $j \neq i$. For any $t \in [0, 1]$, the opened chain $A'(t) = \langle a^*(t), a'_{i+1}(t), a'_{i+2}(t), \ldots, a'_{n-1}(t), a'_0(t), a'_1(t), \ldots, a'_i(t) \rangle$ at time t is obtained from A by fixing $a'_i(t) = a_i$, fixing $a'_{i-1}(t) = a_{i-1}$, and opening each interior angle α_j, $j \neq i$, to $\alpha'_j(t) = \alpha_j + \delta_j(t)$. The opening separates two copies of a_i; we call the stationary copy a_i and the moving copy $a^*(t)$. Because $\delta_j(0) = 0$, the opening motion starts at $A'(0) = A$. Because $\delta_j(t)$ is non-strictly increasing, the interior angles $\alpha'_j(t)$ only open
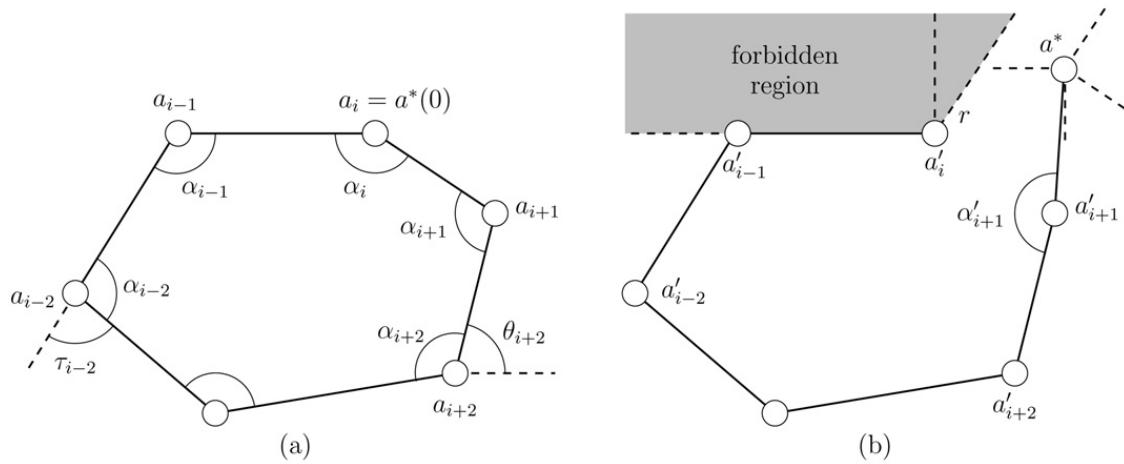
Fig. 5. (a) A convex closed chain A, and (b) an opening of α_{i+1}.

with t. Because $\delta_j(t) \leqslant \tau_j$, the interior angle $\alpha'_j(t)$ remains at most $\alpha_j + \tau_j = \pi$, so the opened chain $A'(t)$ has only right turns. Thus these chains $A'(t)$ can use the same definitions of interior angle $\alpha'_j(t)$, turn angle $\tau'_j(t)$, and counterclockwise angle $\theta'_j(t)$ at a vertex $a'_j(t)$, $j \neq i$, and the analog of Eq. (1) still holds.

Lemma 2. *During any opening $A'(t)$ of a convex closed chain A at a_i, every edge $a'_k(t)a'_{k+1}(t)$ turns clockwise in the sense that the vector $a'_{k+1}(t) - a'_k(t)$ rotates only clockwise as t increases; in particular, $a^*(t)a_{i+1}(t)$ turns clockwise.*

Proof. The transformation of an edge $a_{k-1}a_k$ of A to $a'_{k-1}(t)a'_k(t)$ induced by the opening at time t can be expressed as a composition of rotations, rotating clockwise by $\delta_j(t)$ around each vertex a_j for $j = k, k+1, \ldots, i-1$. In particular, the vector $a'_k(t) - a'_{k-1}(t)$ is a rotation of $a_k - a_{k-1}$ clockwise by $\sum_{j=k}^{i-1} \delta_j(t)$. Because $\delta_i(t) \geqslant 0$ and $\delta_i(t)$ only increases with t, $a_{k+1}(t) - a_k(t)$ rotates only clockwise as t increases. $\square$

Lemma 3. *During any opening $A'(t)$ of a convex closed chain A at a_i, the Euclidean distance between any two vertices $a'_j(t)$ and $a'_k(t)$ only increases with t.*

Proof. Cauchy's arm lemma [8,10] states that opening the interior angles $\alpha_1, \alpha_2, \ldots, \alpha_{n-1}$ of a convex open chain $a_0, a_1, \ldots, a_n$ non-strictly increases the Euclidean distance between the endpoints a_0 and a_n. The lemma follows from applying Cauchy's arm lemma to the chain $a_j, a_{j+1}, \ldots, a_k$ or the chain $a_k, a_{k+1}, \ldots, a_j$, whichever excludes the missing edge $a_i a^*$. $\square$

We define three classes of shapes that an open chain $A' = \langle a^*, a'_{i+1}, a'_{i+2}, \ldots, a'_{n-1}, a'_0, a'_1, \ldots, a'_i \rangle$ with only right turns may have: convex, weakly convex, and spiral. Refer to Fig. 6. The chain A' is *convex* if joining the endpoints a'_i and a^* with a closing segment yields a convex polygon. The chain A' is *weakly convex* if joining the endpoints a'_i and a^* with a segment yields a non-convex simple polygon with no exterior angles smaller than $\pi/2$. Such a weakly convex chain is called *R-weakly convex* or *L-weakly convex* depending on which endpoint is on the hull: if a'_i is on the hull, then the chain is L-weakly convex; if a^* is on the hull, then the chain is R-weakly convex. If the chain A' is neither convex nor weakly convex, then it is a *spiral*.

Lemma 4. *During any opening $A'(t)$ of a convex closed chain A at a_i, $A'(t)$ remains convex or weakly convex, and the endpoint $a^*(t)$ remains outside the normal cone of a_i.*

Proof. Define the *forbidden region* to be the normal cone of a_i unioned with the quarter-plane above the horizontal ray emanating leftward from a_i; see Fig. 5. Initially, no vertex a_j is inside the forbidden region. By Lemma 3, no vertex $a'_j(t)$ can cross an edge $a'_{k-1}(t)a'_k(t)$, for to cross the edge, $a'_j(t)$ would have to approach one of the edge's endpoints. In particular, no vertex $a'_j(t)$ can cross the edge $a_{i-1}a_i$. Because the opened chain $A'(t)$ has only right turns, the only
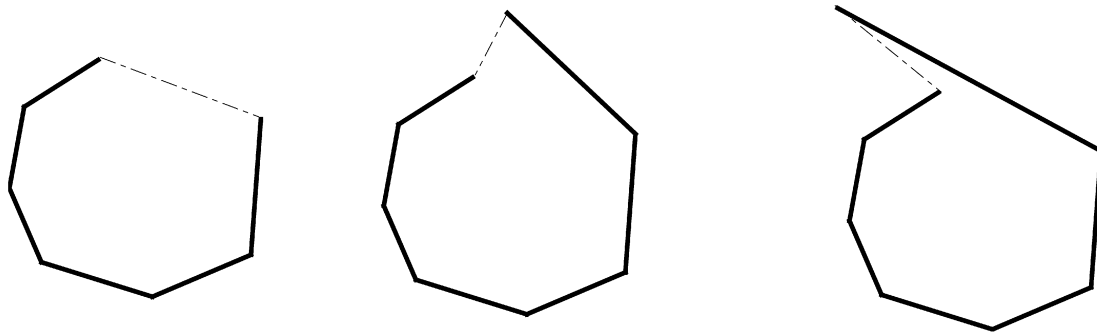
Fig. 6. Types of chains, from left to right: convex, R-weakly convex, spiral. Endpoints are joined by dashed line segments.
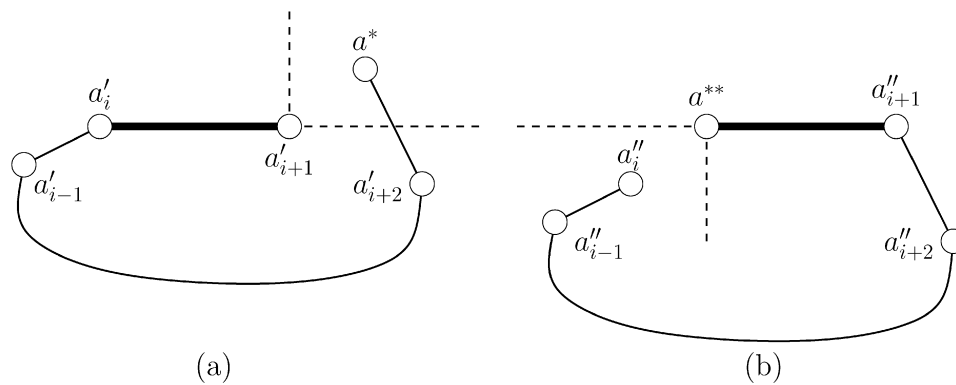

Fig. 7. (a) An opened chain A'. (b) Translating part of the chain to switch the cut vertex. This is a new opened chain A'' except that the angle α_{i+1} is not yet opened.

way for a vertex $a'_j(t)$ of the chain to enter the forbidden region is for $a^*(t)$ to cross the ray r emanating from a_i normal to $a_i a_{i+1}$. Such penetration is possible only when $a^*(t)$ is above or on the horizontal line through the edge $a_{i-1} a_i$, so we consider values of t for which this is the case.

We claim that, for such values of t, the direction of the edge $a^*(t)a'_{i+1}(t)$ remains in the clockwise range from the direction of $a_i a_{i+1}$ to the horizontal leftward direction. By Lemma 2, the edge turns clockwise from its original direction of $a_i a_{i+1}$. If the direction were ever to reach horizontal leftward, it would be impossible to connect $a'_{i+1}(t)$ to a_{i-1} by only turning right and using a total turn angle less than 2π. (Turn angles only decrease while opening, and the initial total turn angle excluding a_i is less than 2π.) The vertices $a'_j(t)$ thus remain in the clockwise wedge around $a^*(t)$ from the direction of $a_i a_{i+1}$ to horizontal leftward. These vertices are the possible centers of a clockwise rotation affecting $a^*(t)$. The resulting instantaneous direction of motion of $a^*(t)$ is thus in the clockwise range from the direction of the normal ray r to vertical downwards (the previous cone of directions rotated clockwise by $\pi/2$). Furthermore, in the case of instantaneous motion along the direction of r, the actual motion of $a^*(t)$ is clockwise of the direction of r. Therefore, $a^*(t)$ moves away from the ray r for these values of t, so it could never cross r.   □

Lemma 5. *Let $A'(t)$ and $A''(t)$ be openings of a convex closed chain A at a_{i+1} and at a_i, respectively, with the same angle-opening $\delta_j(t)$ functions for $j \neq i, i+1$. If $A'(t)$ is R-weakly convex, then $A''(t)$ cannot be L-weakly convex.*

Proof. Because the lemma concerns only a single time t, we omit the t argument. We apply a series of transformations that transform A' into A''; refer to Fig. 7. Because A' is R-weakly convex, a^* must be in the upper-right quadrant of a'_{i+1}. Now we make a new cut at a'_i, and translate the entire opened chain, except the fixed edge $a_i a_{i+1}$, so that a^* re-attaches to a'_{i+1}. We let a''_i denote the translated copy of a'_i, and let $a^{**}a''_{i+1}$ denote the original fixed edge. Now a''_i must be in the lower-left quadrant of a^{**}.

Now we have a new opened chain, except that we have not taken care of the opening of angles α''_i and α''_{i+1}. Because A' opened the angle at a'_i by rotating the chain that we merely translated, and a''_i no longer has an angle to open, we must rotate the translated chain to return it to the original orientation. This rotation is counterclockwise,

because the opening rotation at a_i' was clockwise. Next, because a_{i+1}'' (previously a^*) has an angle not present in A', we must open that angle by again rotating the entire translated chain. Again the rotation is counterclockwise to open a_{i+1}''. (Technically, we should also rotate the entire chain to make $a_{i-1}'' a_i''$ horizontal, but this does not change weak convexity.) During these counterclockwise rotations, a_i'' might cross into the lower-right quadrant of a^{**}, but a_i'' cannot cross into the upper-left quadrant of a^{**}. Therefore cutting at a_i cannot produce an L-weakly convex chain. □

5. Unfolding nested bands

Having completed our study of unfolding cut chains, we now return the original problem of unfolding bands. Our results on chains help understand the motions of the top boundary A and the bottom B of the band. The rest of our study focuses on the cut edge, which can cause intersection as in Fig. 2 if we are not careful.

After cutting a single hinge, a *flattening motion* is a continuous motion during which each face moves rigidly but remains connected to each adjacent face via their common hinge, and the final configuration is planar. If no intersection occurs during the motion, then this motion is a *continuous unfolding*. If the resulting configuration is non-self-intersecting, but intersection occurs during the motion, then we call the motion an *instantaneous unfolding* and the resulting configuration an *unfolded state*. Thus in Fig. 2 we would say that the band has been flattened, but because it self-intersects it has not unfolded. These notions can be defined precisely by specifying rigid motions of the faces as functions of time that satisfy the connectivity constraints, similar to openings of chains.

We now describe the particular flattening motion that will lead to our unfolding, though it requires some effort to prove non-intersection, particularly of the final state. The flattening motion is based on *squeezing* together the two parallel planes $z = z_A$ and $z = z_B$ that contain A and B, keeping the planes parallel and keeping each chain on its respective plane. At time $t \in [0, 1]$, the squeezing motion reduces the vertical separation between the two parallel planes down to $(1 - t)(z_A - z_B)$, that is, it linearly interpolates the separation from the original $z_A - z_B$ down to 0.

The squeezing uniquely determines the hinge dihedral angles necessary to keep the vertices of the band on their respective moving planes (assuming exactly one edge of the band has been cut). See Fig. 8 for an example of the projected motion. For nested bands, the motion increases the interior angle at every vertex of each chain in projection. This property can be seen by examining any two adjacent faces that are being "squeezed". Both faces rotate continuously to become more horizontal. If we forced one of the faces to keep its vertices in the parallel planes, but allow the second face to only follow this motion rigidly (i.e., the dihedral angle at the hinge remains fixed), then the edges of the second face would no longer be on the horizontal planes. To compensate, the second face must perform a (dihedral) rotation about the hinge. In fact, the interior angle at the hinge must increase (flatten), causing the interior
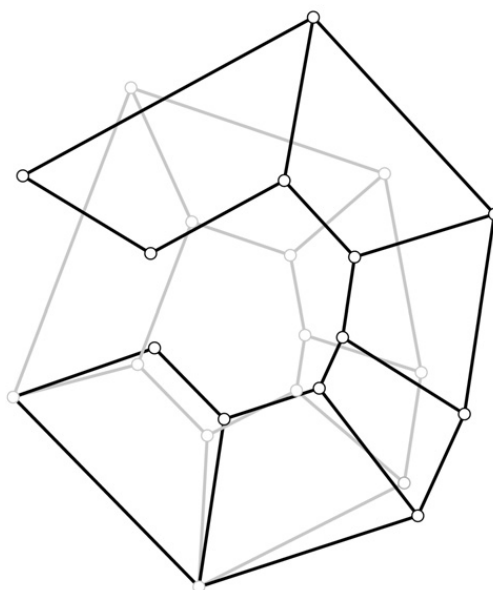

Fig. 8. A view from above of a nested band during a squeezing motion. The original configuration has a lighter shade. For each trapezoid, the height increases and its parallel edges rotate clockwise relative to their original positions.
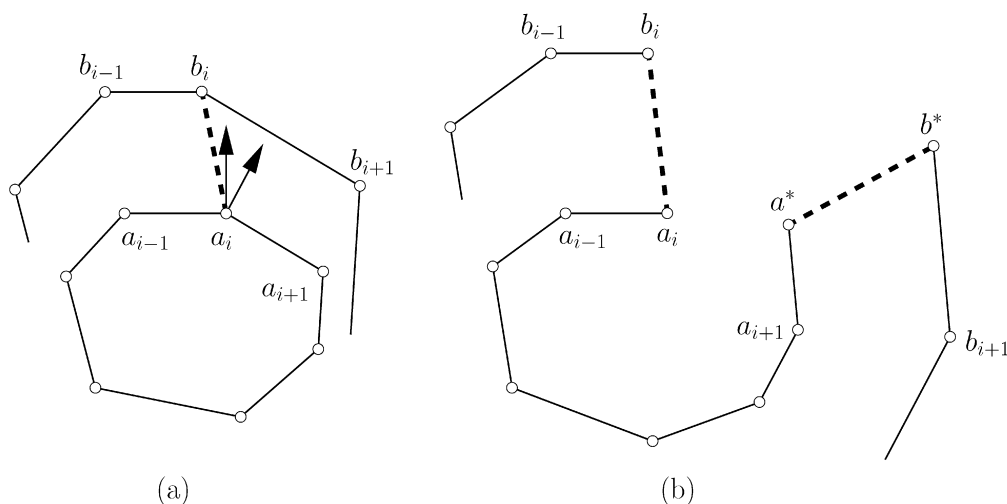
Fig. 9. (a) Projection of the inner convex chain A and part of the outer chain B. Hinge $a_i b_i$ and the normal cone of vertex a_i are shown. (b) The result of cutting at $a_i b_i$ and flattening.

angles of the chains to increase (open). Because the interior angle at a vertex of a nested band can open only to π, the opening chain will always have only right turns. Thus we can apply the analysis of opening chains from Section 4. For example, Lemma 4 tells us that the opening chains never become spirals, so in particular never self-intersect while flattening (a fact already known from the slice-curve result of [8,10]).

As the parallel planes squeeze together, each band face remains a trapezoid in the projection. Edges $a_i a_{i+1}$ and $b_i b_{i+1}$ remain parallel and retain their original lengths throughout. Hinge projections lengthen as the band is squeezed, which causes the trapezoid angles to change. Because b_i and b_{i+1} move orthogonally away from $a_i a_{i+1}$, acute trapezoid angles increase toward $\pi/2$ and obtuse angles decrease toward $\pi/2$.

The goal of this section is to show that the band does not self-intersect if we cut a specific hinge. We mention that self-intersection of the band in 3D implies self-intersection in projection, so it suffices to prove that there is no self-intersection in projection to establish that there is no self-intersection in 3D.

Suppose that we cut hinge $a_i b_i$ and hold $a_{i-1} a_i$ fixed along the x axis in the positive direction. The motion separates two copies of a_i; we call the stationary one a_i, and call the moving one a^*, as in Fig. 5. Correspondingly, for the outer chain, the direction of $b_{i-1} b_i$ remains fixed (it moves away from $a_{i-1} a_i$ because the trapezoid enlarges in projection, but remains parallel), and b^* is a "moving" endpoint. Thus the cut hinge is split into edges $a_i b_i$ and $a^* b^*$. See Fig. 9.

Call a chain A *safe* if it is either convex, or it is R-weakly convex and the hinge $a_i b_i$ is left of or in the normal cone at a_i, or it is L-weakly convex and $a_i b_i$ is right of or in the normal cone at a_i. An opening of the band is *safe* if the opened inner chain A is safe. See Fig. 10. We will prove that safe openings of the band never self-intersect, i.e., are unfoldings. Then we will prove that there is always a suitable hinge $a_i b_i$ that leads to a safe opening.

Our next lemma covers an opened band by a clockwise-turning family of rays emanating from the inner chain A, dependent only on the cut edges and not on the outer chain B. This covering will allow us to prove non-overlap of the opened band—in fact, an infinite version of the band with no bounding outer chain—in certain cases using the non-overlap of A.

Lemma 6. *For any safe opening of the band, there is a function r assigning a ray $r(p)$ from each point p on the chain A such that*

(1) *r is a continuous function*;
(2) *the direction of $r(p)$ rotates only clockwise as p moves along A from a^* to a_i*;
(3) *the total turn angle made by $r(p)$ as p travels along A from a^* to a_i is at most 2π*;
(4) *the ray $r(p)$ is locally exterior to the polygon formed by A and the edge $a_i a^*$; and*
(5) *the ray $r(a_i)$ passes through b_i, and the ray $r(a^*)$ passes through b^*.*

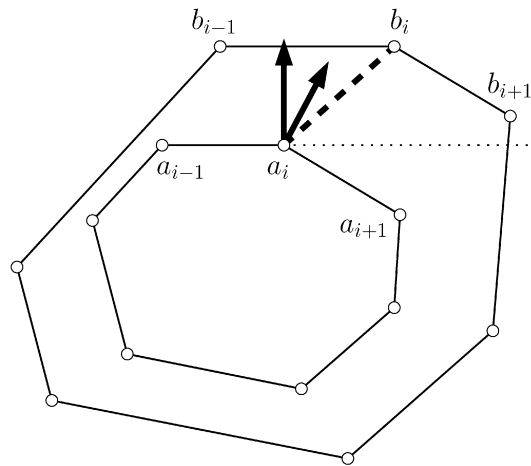(*Only Property* 4 *requires safeness*.)

Fig. 10. After cutting at a_i, the inner chain will become R-weakly convex if a^* ends up above the line determined by $a_{i-1}a_i$ (dotted). In this case, the cut is labeled *safe* if hinge a_ib_i (dashed) is left of or in the normal cone at a_i (which is not the case in this figure).

Proof. First we assign $r(a_j)$ for each vertex a_j. We set $r(a_i)$ to the ray from a_i passing through b_i, and set $r(a^*)$ be the ray from a^* passing through b^*. Thus we obtain Property 5 For each $j \neq i$, let $[u_j, w_j]$ denote the clockwise range of directions of rays that are left of the two incident edges $a_{j-1}a_j$ and a_ja_{j+1} (and hence locally exterior to A). We set the direction of $r(a_j)$, $j \neq i$, according to three cases:

(1) If the direction of $r(a_i)$ is in the clockwise range $[u_j, w_j]$, then we set the direction of $r(a_j)$ to the direction of $r(a_i)$.
(2) Otherwise, if the direction of $r(a^*)$ is in the clockwise range $[u_j, w_j]$, then we set the direction of $r(a_j)$ to the direction of $r(a^*)$.
(3) Otherwise, we set the direction of $r(a_j)$ to the direction in the middle of the range $[u_j, w_j]$, i.e., $r(a_j)$ is the angular bisector of the exterior (non-convex) angle at a_j.

Finally, we make r a continuous function over points on A by linearly interpolating the direction from $r(a_{j-1})$ to $r(a_j)$ for points along the edge $a_{j-1}a_j$, keeping the rays left of the edge. Thus we obtain Property 1.

Next we show Property 2 for the points along any edge $a_{j-1}a_j$. We split into three cases. If $r(a_{j-1})$ and $r(a_j)$ are exterior angular bisectors of a_{j-1} and a_j, respectively, then the claim follows because the exterior angles are non-convex, so $r(a_{j-1})$ is left of the edge normal (at a_{j-1}), while $r(a_j)$ is right of the edge normal (at a_j). If $r(a_{j-1})$ has the same direction as $r(a^*)$, then $r(a_{j-1})$ must be strictly left of the line from a_{j+1} to a_j (in direction), while $r(a_j)$ is non-strictly right of this line, so the claim follows. The case when $r(a_j)$ has the same direction as $r(a_i)$ is symmetric. Thus we obtain Property 2.

Next we show Property 3. Along each edge $a_{j-1}a_j$ of A for which $r(a_{j-1})$ and $r(a_j)$ are angular bisectors, the ray turns $\frac{1}{2}(\tau_{j-1} + \tau_j)$: $\frac{1}{2}\tau_{j-1}$ turn from $r(a_{j-1})$ to a normal to $a_{j-1}a_j$, and $\frac{1}{2}\tau_j$ turn from that normal to $r(a_j)$. Thus the total turn caused by such edges is at most $\frac{1}{2}\sum_{j \neq i,i+1}(\tau_{j-1} + \tau_j) = \sum_j \tau_j - \tau_i - \frac{1}{2}(\tau_{i-1} + \tau_{i+1})$. In the original chain A before opening, the total turn angle $\sum_j \tau_j$ is 2π, and opening the chain only decreases the turn angle τ_j at each vertex a_j, so $\sum_j \tau_j$ remains at most 2π. Thus the total turn of ray from being normal to a^*a_{i+1} to being normal to $a_{i-1}a_i$, visiting the angular bisectors of a_j, $j \neq i$, in between, is at most $2\pi - \tau_i$. If the projected trapezoid angle at a_i ($\angle a_{i-1}a_ib_i$) is acute, then this total turn has already accounted for reaching (in fact, going beyond) the direction of ray $r(a_i)$; if the angle is obtuse, however, then we must also add the clockwise angle from the normal of $a_{i-1}a_i$ to $r(a_i)$ to the total turn. Similarly, if the projected trapezoid angle at a^* ($\angle b^*a^*a_{i+1}$) is obtuse, then we must add the clockwise angle from $r(a^*)$ to the normal of a^*a_{i+1} to the total turn. Before the opening, the sum of these two clockwise angles is τ_i, and the flattening of the trapezoids only decreases these projected angles. Thus, the additional turn remains at most τ_i. The total turn angle of the rays is therefore at most 2π, proving Property 3.

Finally we show Property 4. The property holds along any edge $a_{j-1}a_j$ of A, with respect to that edge, because rays $r(a_{j-1})$ and $r(a_j)$ are both chosen to be left of the edge $a_{j-1}a_j$, and because by Property 2, $r(a_j)$ is clockwise of $r(a_{j-1})$ in the halfplane left of $a_{j-1}a_j$. It remains to show Property 4 at a_i and a^* with respect to the closing edge
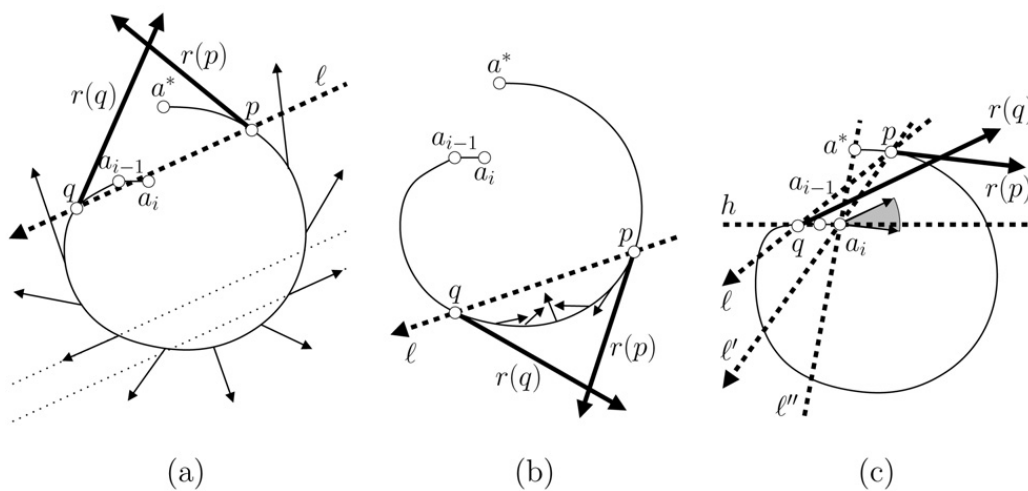
Fig. 11. Three cases of rays $r(p)$ and $r(q)$ attempting to cross.

$a_i a^*$. Assume without loss of generality that A is either convex or R-weakly convex. (Otherwise, imagine opening from the other side, swapping the roles of a_i and a^*.) In either case, $a^* a_{i+1}$ is an edge of the convex hull of A. Because the incident projected trapezoid of the band is left of this edge, $a^* b^*$ and hence $r(a^*)$ are left of this edge. Thus $r(a^*)$ is exterior to A. For convex chains, the same argument shows that $r(a_i)$ is left of the edge $a_{i-1} a_i$ and hence exterior to A, completing the proof in this case. Now consider R-weakly convex chains. By safeness, $a_i b_i$ and hence $r(a_i)$ is left of or in the normal cone at a_i. By Lemma 4, a^* is right of this normal cone. Hence, $r(a_i)$ is locally outward with respect to the edge $a_i a^*$. Therefore, in all cases, we have Property 4. $\quad\square$

Lemma 7. *For any ray assignment r on a safe opened chain A satisfying Properties* 1–5 *of Lemma* 6, *no two rays $r(p)$ and $r(q)$ intersect for two points $p \neq q$ of A.*[8]

Proof. Consider any two points p and q on A, and assume by symmetry that q appears after p in the clockwise order around A. Let ℓ be the directed line from p to q. For the rays $r(p)$ and $r(q)$ to intersect, they have to be on the same side of ℓ.

Suppose first that $r(p)$ and $r(q)$ are both right of ℓ, as in Fig. 11(a). For these rays to intersect, $r(q)$ must be clockwise of $r(p)$ in the halfplane right of ℓ. As we move a point x from p to q clockwise around A, $r(x)$ must rotate continuously clockwise by Properties 1 and 2 of Lemma 6. During this motion, $r(x)$ sweeps the clockwise angle from $r(p)$ to the reverse direction of ℓ, then it sweeps the π clockwise angle from the reverse direction of ℓ to the forward direction of ℓ, and finally it sweeps the clockwise angle from the forward direction of ℓ to $r(q)$. If $r(p)$ is counterclockwise of $r(q)$ in the halfplane right of ℓ, the first and last angle must overlap, summing to more than π, and hence $r(x)$ must sweep an angle more than 2π during x's motion, contradicting Property 3 of Lemma 6. Therefore $r(p)$ and $r(q)$ cannot intersect right of ℓ.

It remains to consider the case when both $r(p)$ and $r(q)$ are left of ℓ. For these rays to intersect, $r(p)$ must be clockwise of $r(q)$ in the halfplane left of ℓ. As a first subcase, suppose that the entire subchain of A from p to q is non-strictly left of ℓ, as in Fig. 11(b); in particular, this subcase happens when A is convex. As in the previous case, if we move a point x from p to q clockwise around A, $r(x)$ must rotate continuously clockwise by Properties 1 and 2 of Lemma 6. If $r(p)$ is clockwise of $r(q)$ in the halfplane left of ℓ, then $r(x)$ must at some point locally enter the polygon, contradicting Property 4 of Lemma 6. Hence $r(p)$ and $r(q)$ cannot intersect in this subcase.

We are left with the subcase when A is weakly convex and the subchain of A between p and q is at some point right of ℓ, as in Fig. 11(c). This last property implies that ℓ intersects A between p and q. Assume without loss of generality that A is R-weakly convex, and thus a^* is above the horizontal line h through $a_{i-1} a_i$. (Otherwise, imagine opening from the other side, swapping the roles of a_i and a^*.) Now h partitions the chain A into two convex subchains, where the subchain above h precedes the subchain below h in the clockwise order of A. For ℓ to intersect A between

---

[8] Thereby avoiding total protonic reversal [11].

p and q, p and q must be on opposite sides of h, and by the clockwise ordering, p must be above h and q must be below (or on) h. By R-weak convexity, both a^* and p are in the upper-right quadrant from a_i. In particular, the line ℓ'' through the closing edge $a_i a^*$ and the line ℓ' through a_i and p both have positive slope. Now ℓ' partitions the portion of A clockwise after p into two convex subchains, and if we direct ℓ' from p to a_i, the subchain non-strictly left of ℓ' contains p. For ℓ to intersect A between p and q, q must be on the subchain right of ℓ', which is in the lower-left quadrant of a_i. Hence, the slope of ℓ must be positive and at most the slope of ℓ'. (Note that the slope of a line does not depend on the line's orientation.) Furthermore, the slope of ℓ' is at most the slope of ℓ''. By Properties 1, 2, and 3 of Lemma 6, the direction of $r(a_i)$ must be in the clockwise range from the direction of $r(q)$ to the direction of $r(p)$. In particular, this cone of directions is in the halfplane left of ℓ. By the slope arguments above, this cone is contained in the non-convex clockwise wedge from the ray starting at a_i through a^* to the horizontal leftward ray starting at a_i. But then $r(a_i)$ locally enters the polygon, contradicting Property 4 of Lemma 6. □

Lemma 8. *For any ray assignment r on a safe opened chain A satisfying Properties 1–5 of Lemma 6, the union of rays $r(p)$ over all points p on A covers the opened band.*

Proof. The chains A and B, together with the hinges $a_i b_i$ and $a^* b^*$, define a bounded but possibly self-intersecting polygon, namely, the opened band. For each point p on A, let $b(p)$ denote the first point of the boundary of this polygon that is intersected by the ray $r(p)$. By boundedness of the polygon, the ray $r(p)$ must exit the band. By Property 4 of Lemma 6, $r(p)$ cannot immediately exit at p; and by Lemma 7, $r(p)$ cannot exit by intersecting A at any other point q because then $r(p)$ would intersect $r(q)$. By Lemma 7, $r(p)$ cannot exit by intersecting either of the hinges, because then it would intersect $r(a_i)$ or $r(a^*)$. Thus, $r(p)$ must exit the polygon by intersecting B at some point $b(p)$.

By Property 1 of Lemma 6, $b(p)$ varies continuously along B. By Lemma 7, $b(p) \neq b(q)$ for any two points $p \neq q$ of A. By Lemma 5, $b(a_i) = b_i$ and $b(a^*) = b^*$. Thus, as we vary p along A from a^* to a_i, $b(p)$ varies continuously and monotonically along B from b^* to b_i. At any point p during this motion, the ray $r(p)$ covers the segment $pb(p)$ contained by the band. These segments define a *ruling* of the band, starting at $a^* b^*$, ending at $a_i b_i$, and in between moving along the two other boundary chains A and B.

The consequence is that the continuum of segments $pb(p)$, and hence the containing rays $r(p)$, cover the band. This consequence can be seen perhaps more clearly by dividing the ruling at the finitely many key positions when p is a vertex of A or $b(p)$ is a vertex of B. Then we effectively divide the problem into the regions of time between these key positions, where we simply have a linear ruling of a quadrangle. □

Combining Lemmas 7 and 8, we obtain the following important consequence:

Corollary 9. *Any safe opening of a band does not self-intersect.*

Now we turn to proving that a safe opening always exists. By Lemma 1, there is a vertex a_k whose hinge is counterclockwise of the normal cone at a_k, while the hinge at a_{k+1} is clockwise of its respective cone. For the cuts at both vertices to produce unsafe inner chains, cutting at a_k must produce an L-weakly convex chain, while cutting at a_{k+1} must produce an R-weakly convex chain. See Fig. 12.
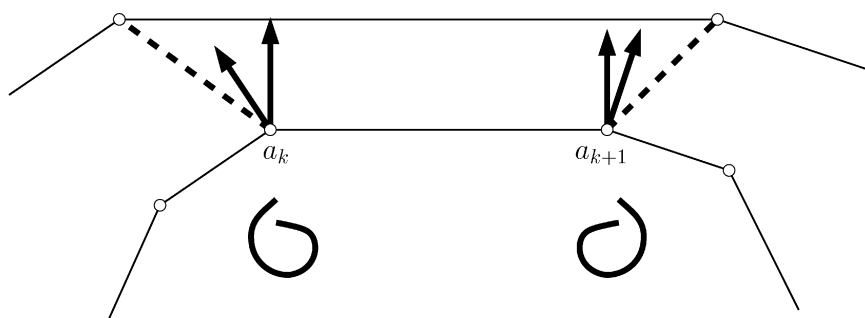

Fig. 12. Two successive vertices, a_k and a_{k+1}, whose cuts produce different weakly convex chains (indicated by the curves below the vertices).

But by Lemma 5, this situation is impossible. Thus, we can always find a suitable vertex to cut so that the inner chain opens to a safe position, which by Corollary 9 implies that we can always find an edge to cut along so that a nested band has an unfolded state. This completes the proof of our main result:

Theorem 10. *Every nested band has an unfolded state.*

The non-intersection of the final state turns out to be the main challenge for our unfolding motion, and we can use it to establish non-intersection throughout:

Theorem 11. *Every nested band has a continuous unfolding motion.*

Proof. The squeezing motion that we have defined has the property that all the points with the same original height have the same new height at any time t during the squeezing motion, and vice versa for $t < 1$. To see this, parameterize a point p on the band by its original height z_p divided by the height z of the original band. After partially squeezing the band to height z_s, the new height of p will be $z_s(z_p/z)$.

Now, suppose that two points p and q intersected at some time $t < 1$ during the squeezing motion. At this time, the points have the same height, so at their original positions at time 0, p and q must also have the same height h. We can view the motion of p and q as the development of a slice curve $z = h$. But by the results of [8,10], p and q can never intersect.

We conclude that no intersection can occur until the final flattened configuration of the band, which is a singularity where the above arguments do not apply. By Theorem 10, there is a cut that produces an unfolded state. Therefore, by making the same cut and applying the squeezing motion, we obtain a continuous unfolding of the band. □

6. Remarks

We note that another natural continuous unfolding motion exists, consisting of $n - 1$ peeling moves. After cutting a hinge that produces an unfolded state, we begin by performing a dihedral rotation about its neighboring hinge, so that two trapezoids become coplanar. Subsequent moves are simple dihedral rotations about successive hinges, and each step adds one more trapezoid to the coplanar subset. Because this motion is not necessary for our results on nested bands, a detailed proof of its correctness is omitted. We mention it, though, because follow-on work establishes that this motion unfolds non-nested bands, even those that contain polyhedron vertices on their boundaries [1].

Even with it established that arbitrary bands can be unfolded without overlap, it remains interesting to see whether this can lead to a non-overlapping unfolding of prismatoids, including the top and bottom faces. It is natural to hope that these faces could be nestled on opposite sides of the unfolded band, but we do not know how to ensure non-overlap.

Acknowledgements

References

[1] G. Aloupis, Reconfigurations of polygonal structures, Ph.D. Thesis, McGill University, March 2005.
[2] G.A. Arteca, P.G. Mezey, A method for the characterization of foldings in protein ribbon models, J. Mol. Graph. 8 (June 1990) 66–80.
[3] P. Bhattacharya, A. Rosenfeld, Polygonal ribbons in two and three dimensions, Pattern Recognition 28 (5) (1995) 769–779.
[4] C. Borcea, I. Streinu, Singularities of hinge structures, in: Effective Methods in Algebraic Geometry, Porto Conte, Sardinia, May 2005.
[5] H.M. Cundy, A.P. Rollett, Mathematical Models, Oxford University Press, 1961.
[6] E.D. Demaine, J. O'Rourke, Geometric Folding Algorithms: Linkages, Origami, Polyhedra, Cambridge University Press, 2007.

[7] E.D. Demaine, J. O'Rourke, A survey of folding and unfolding in computational geometry, in: J.E. Goodman, J. Pach, E. Welzl (Eds.), Combinatorial and Computational Geometry, in: Mathematical Sciences Research Institute Publications, vol. 52, Cambridge University Press, August 2005, pp. 167–211.

[8] J. O'Rourke, On the development of the intersection of a plane with a polytope, Comput. Geom. Theory Appl. 24 (1) (2003) 3–10.

[9] J. O'Rourke, Folding and unfolding in computational geometry, in: Discrete Comput. Geom., in: Lecture Notes Comput. Sci., vol. 1763, Springer-Verlag, 2000, pp. 258–266. Papers from the Japan Conf. Discrete Comput. Geom., Tokyo, December 1998.

[10] J. O'Rourke, An extension of Cauchy's arm lemma with application to curve development, in: Discrete Comput. Geom., in: Lecture Notes Comput. Sci., vol. 2098, Springer-Verlag, 2001, pp. 280–291. Papers from the Japan Conf. Discrete Comput. Geom., Tokyo, November 2000.

[11] I. Reitman (director), D. Akroyd, H. Ramis (writers), Ghost Busters, Colombia Pictures, 1984.

[12] G.C. Shephard, Convex polytopes with convex nets, Math. Proc. Cambridge Philos. Soc. 78 (1975) 389–403.

[13] W. Whiteley, Rigidity of molecular structures: generic and geometric analysis, in: M.F. Thorpe, D.M. Duxbury (Eds.), Rigidity Theory and Applications, Kluwer Academic, 1999, pp. 21–46.